Conference on Modelling Fluid Flow (CMFF'22)
The 18th International Conference on Fluid Flow Technologies
Budapest, Hungary, August 30-September 2, 2022

COMPARISON STUDY OF THE $k - k_L - \omega$ AND $\gamma - Re_\theta$ TRANSITION MODELS IN THE OPEN WATER PERFORMANCE PREDICTION OF A RIM-DRIVEN THRUSTER

Bao LIU[1], Maarten VANIERSCHOT[2], Frank BUYSSCHAERT[3]

[1] Department of Mechanical Engineering, Group T Leuven Campus, KU Leuven, Leuven, Belgium. E-mail: bao.liu@kuleuven.be
[2] Corresponding Author. Department of Mechanical Engineering, Group T Leuven Campus, KU Leuven, Leuven, Belgium. E-mail: maarten.vanierschot@kuleuven.be
[3] Department of Mechanical Engineering, Bruges Campus, KU Leuven, Bruges, Belgium. E-mail: frank.buysschaert@kuleuven.be

ABSTRACT

The present work examines the capabilities of two transition models implemented in ANSYS Fluent in the open water performance prediction of a rim-driven thruster (RDT). The adopted models are the three equation $k - k_l - \omega$ and the four equation $\gamma - Re_\theta$ models. Both models are first tested on a ducted propeller. The numerical results are compared with available experimental data and a good correlation is found for both. Simulations employing both transition models are then carried out on a four-bladed rim-driven thruster model and the results are compared with the $k - \omega$ SST turbulence model. It is observed that the streamline patterns on the blade surface are significantly different between the transition and fully turbulent models. The transition models can reveal a laminar region on the blade while the $k - \omega$ SST model assumes the flow is entirely turbulent, resulting in a considerable difference in torque prediction. It is noted that unlike the $k - \omega$ SST model, the transition models are quite sensitive to the free stream turbulence quantities such as turbulent intensity and turbulent viscosity ratio, as these quantities determine the onset of the transition process. Finally, the open water performance of the RDT and the structure of the flow field are also presented and discussed.

Keywords: transition model, rim-driven thruster, open water performance

NOMENCLATURE

δ_{ij}	$[-]$	Kronecker delta
ϵ	$[m^2/s^3]$	dissipation rate of turbulent kinetic energy
γ	$[-]$	intermittency
Re	$[-]$	Reynolds number
Re_θ	$[-]$	momentum thickness Reynolds number
$\mathrm{Re}_{\theta t}$, $\widetilde{\mathrm{Re}}_{\theta t}$	$[-]$	transition onset momentum thickness Reynolds number
μ	$[kg/(m \cdot s)]$	dynamic viscosity
μ_t	$[kg/(m \cdot s)]$	turbulent or eddy viscosity
ν	$[m^2/s]$	kinematic viscosity
ω	$[1/s]$	specific dissipation rate of turbulent kinetic energy
ρ	$[kg/m^3]$	fluid density
$\rho\overline{u_i'u_j'}$	$[N/m^2]$	Reynolds stress
τ_w	$[N/m^2]$	wall shear stress
C_f	$[-]$	skin friction coefficient
C_p	$[-]$	pressure coefficient
D	$[m]$	propeller diameter
d	$[m]$	wall distance
J	$[-]$	advance coefficient
k/k_T	$[m^2/s^2]$	turbulent kinetic energy
K_{Qp}	$[-]$	propeller torque coefficient
K_{Qr}	$[-]$	rim torque coefficient
K_{Td}	$[-]$	duct thrust coefficient
K_{Tp}	$[-]$	propeller thrust coefficient
K_{Tr}	$[-]$	rim thrust coefficient
k_L	$[m^2/s^2]$	laminar kinetic energy
n	$[1/s]$	rotational speed
p	$[Pa]$	dynamic pressure
v	$[m/s]$	representative velocity
v_a	$[m/s]$	advance velocity

Subscripts and Superscripts

PS, SS	pressure side, suction side
T, Q	thrust, torque

1. INTRODUCTION

Computational Fluid Dynamics (CFD) has become a very powerful tool in analyzing engineering problems in recent decades, such as the performance prediction of marine propellers. The widest application is achieved by solving the Reynolds-Averaged Navier-Stokes (RANS) equations because compared

to other approaches, such as Direct Numerical Simulation (DNS) or Large Eddy Simulation (LES), the RANS method is much cheaper with still a reasonable accuracy. To solve the Reynolds stress terms in the RANS equations, turbulence models based on the Boussinesq hypothesis are introduced. Amongst them, the most popular ones are the $k-\epsilon$ and $k-\omega$ models. Since these turbulence models are built on the assumption that the resolved flow field is fully turbulent, they are incapable of predicting transition phenomena which are frequently encountered in physical problems. In order to improve the potential of the currently existing turbulence models in resolving transitional flows, a lot of efforts have been made to develop models which can predict the transition process from laminar to turbulence. There are generally two approaches: one is to couple transition correlations, which are obtained from available experimental data, into the turbulence models; the other one is to solve additional transport equations to account for the transitional effects. However, even if a transition model is successfully developed, it is still questionable whether it can be implemented into modern CFD codes which are usually based on unstructured grids and parallel execution, as most transition models are still using non-local variables or integral terms. Single-point models which use only local variables are required for general application. In ANSYS Fluent, there are two transition models available, i.e. the three equation $k-k_L-\omega$ and four equation $\gamma-Re_\theta$ models. Both models introduce additional transport equations to include the transitional effects in flows.

The present work aims to test the capabilities of these two transition models in the hydrodynamic characteristics prediction of a rim-driven thruster (RDT). As confirmed in the research of Kuiper [1], for a propeller of model scale, there is often a large area of laminar flow on both sides of the blade surface. In order to investigate the potential reason for discrepancy between simulations and experiments, especially at a high loading condition, Wang [2] employed the Loci/CHEM flow solver to study a marine propeller 5168 using the $k-k_L-\omega$ transition model. The SST $k-\omega$ turbulence model was also used for comparison. The simulation results were analyzed and compared with experimental data. It was found that the transition model showed better performance in resolving the flow field and therefore improved the prediction accuracy, while the standard SST $k-\omega$ model indicated excessive dissipation of vortex cores. Pawar [3] investigated the propeller of an Autonomous Underwater Vehicle (AUV) which often operates at low Reynolds numbers. The global and local hydrodynamic characteristics of an open and ducted propeller are investigated with the $\gamma-Re_\theta$ transition model. The results demonstrated that the transition model was able to predict the complex flow physics such as leading-edge separation, tip leakage vortex, and the separation bubble on the outer surface of the duct.

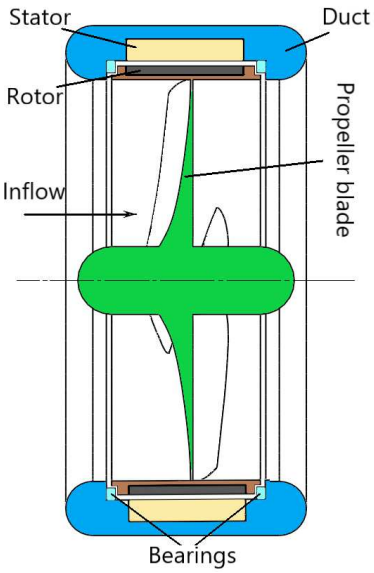

Figure 1. Schematic layout of an RDT

An RDT resembles a ducted propeller in structural design as both contain a propeller and duct. But unlike for a ducted propeller, there is no tip clearance on the RDT propeller. Instead, a gap channel is formed by the rim and duct surfaces. The schematic of an RDT layout is presented in Figure 1 [4]. According whether there is a central hub, the RDT can be roughly classified into the hub type and the hub-less type (Figure 2). Both types have their own advantages and disadvantages [5]. For example, the hub type RDT has a greater structural strength and bearings can be installed in the hub to reduce friction, while the hubless type has a simpler structure and higher hydrodynamic efficiency. Due to the appealing potential the RDT possesses, many researches have been conducted on the modeling and evaluation of RDTs using both fully turbulent RANS models [4, 6, 7, 8, 9, 10] as well as transition models [11]. For the model-scale RDT, the flow on the propeller often tends to be in the laminar or transitional regime. Therefore, transitional modeling is required to better resolve the boundary layer in order to achieve improved hydrodynamic performance prediction. Nevertheless, a detailed comparison between different transition models is still lacking and this study tries to fill this knowledge gap. The structure of the paper is organized as follows: firstly a brief description of the transition models used in this study is presented, then some validation studies are carried out to test the capabilities of those models, followed by the results and discussion of the RDT simulations.

2. NUMERICAL MODELING

The RANS equations for incompressible Newtonian fluids are given as

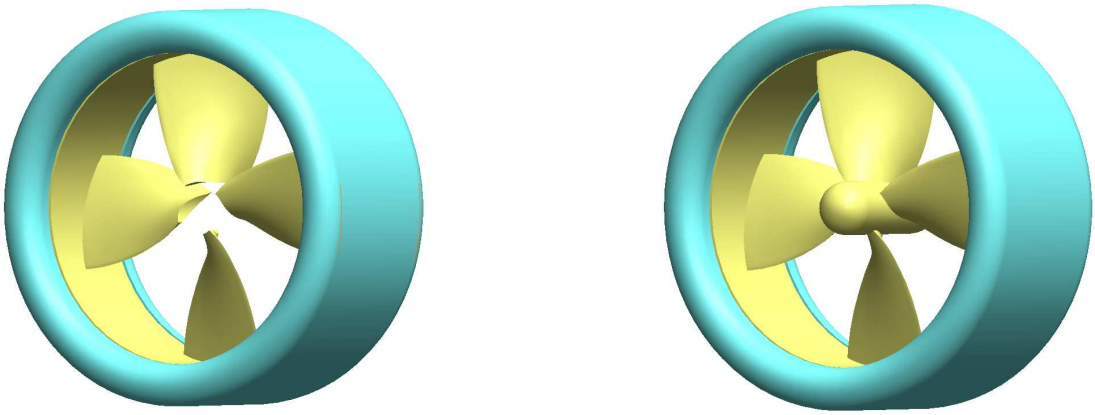

(a) Hub-less type **(b) Hub type**

Figure 2. RDT categorization based on the structural design

$$\frac{\partial u_i}{\partial x_i} = 0, \tag{1}$$

$$\rho\left(\frac{\partial u_i}{\partial t} + u_j\frac{\partial u_i}{\partial x_j}\right) = -\frac{\partial p}{\partial x_i} + \mu\frac{\partial^2 u_i}{\partial x_j \partial x_j} + \frac{\partial}{\partial x_j}\left(-\rho\overline{u_i' u_j'}\right),$$

where ρ is the fluid density, x_i and u_i $(i, j = 1, 2, 3)$ are the spatial coordinate and mean velocity component respectively, t is the flow time, p is the pressure, μ is the dynamic viscosity and $-\rho\overline{u_i' u_j'}$ is the Reynolds stress term. For incompressible Newtonian flows, the Reynolds stress can be related to the mean strain rate and eddy viscosity as follows

$$-\rho\overline{u_i' u_j'} = \mu_t\left(\frac{\partial u_i}{\partial x_j} + \frac{\partial u_j}{\partial x_i}\right) - \frac{2}{3}\rho k\delta_{ij}, \tag{2}$$

where μ_t is the turbulent viscosity, k the turbulent kinetic energy and δ_{ij} the Kronecker delta. The formulation of closure to the above equations is called turbulence modeling. Currently the most popular turbulence models in industrial applications are the two-equation ones, like the $k-\epsilon$ model. This model has gone through many modifications to improve and extend its applicability. It has great capabilities for free-shear flows but behaves poorly in flows with an adverse pressure gradient. To tackle this issue, the $k-\omega$ model by was proposed, which has better performance for flows with weak adverse pressure gradient. Again, several updates have been made to this model to enhance its performance.

2.1. $k-\omega$ SST model

The $k-\omega$ SST turbulence model developed by Menter [12] is an improved version of the original $k-\omega$ model. It has robust near wall treatment and the ability to compute flows with moderate adverse pressure gradients. The transport equations for the turbulent kinetic energy k and the specific turbulent dissipation rate ω are given in [12].

2.2. $\gamma - Re_\theta$ transition model

The $\gamma - Re_\theta$ transition model is a correlation-based transition model using local variables, which contains two additional transport equations, i.e. for the intermittency γ and the transition onset momentum thickness Reynolds number $\widetilde{Re}_{\theta t}$. The additional transport equations are not used to model the transition physics but to provide a framework to which empirical correlations can be made for specific cases. The intermittency is a measure of the flow if it is laminar or turbulent: $\gamma = 0$ means fully laminar flow and $\gamma = 1$ means fully turbulent flow. Therefore, the intermittency equation is used to trigger the local transition process. The second quantity is the transition onset Reynolds number $Re_{\theta t}$, which is used to account for the non-local influence of turbulence intensity on the boundary layer, as well as to relate the empirical correlation to the onset criteria in the intermittency equation. Finally the intermittency function is coupled with the original $k-\omega$ SST model, which is used to turn on the production term of the turbulent kinetic energy downstream of the transition location and the equation for the $\widetilde{Re}_{\theta t}$ can pass the information on the free-stream conditions into the boundary layer. The formulated equations for the intermittency γ and transition momentum thickness Reynolds number $\widetilde{Re}_{\theta t}$ are given as:

$$\rho\left(\frac{\partial \gamma}{\partial t} + \frac{\partial\left(u_j\gamma\right)}{\partial x_i}\right) = P_\gamma - E_\gamma + \frac{\partial}{\partial x_i}\left[\left(\mu + \frac{\mu_t}{\sigma_f}\right)\frac{\partial \gamma}{\partial x_j}\right] \tag{3}$$

$$\rho\left(\frac{\partial \widetilde{\mathrm{Re}}_{\theta t}}{\partial t} + \frac{\partial u_j \widetilde{\mathrm{Re}}_{\theta t}}{\partial x_j}\right) = P_{\theta t} + \frac{\partial}{\partial x_j}\left[\sigma_{\theta t}\left(\mu + \mu_t\right)\frac{\partial \widetilde{\mathrm{Re}}_{\theta t}}{\partial x_j}\right] \tag{4}$$

where P_γ, E_γ are source terms which control the production and destruction of the intermittency, σ_f is a model constant equal to 1, $P_{\theta t}$ is the production term

that is designed to relate the transported scalar $\widetilde{\mathrm{Re}}_{\theta t}$ to the local empirical $\mathrm{Re}_{\theta t}$ outside the boundary layer, and $\sigma_{\theta t}$ is a model constant equal to 10. The detailed definitions of the above terms can be found in [13]. The effective intermittency γ_{eff}, obtained by solving the above equations, is incorporated into the transport equations for k and ω in the $k-\omega$ SST model.

2.3. $k - k_L - \omega$ model

Unlike the $\gamma - Re_\theta$ model, the $k - k_L - \omega$ model is a physics-based model. Three additional transport equations are solved to account for the effects of pre-transition fluctuations, including the bypass and natural transitions. In this model, the concept of laminar kinetic energy k_L is employed, which represents the velocity fluctuations in the pre-transitional regions. With the increase of turbulence intensity in the freestream, the mean velocity profiles in these regions are distorted and more intensive streamwise fluctuations can take place, which finally break down and result in transition. This occurs when the characteristic time-scale for turbulence production is smaller than the viscous diffusion timescale of the pre-transitional fluctuations. It is assumed that the production of k_L is a result of the interaction between the Reynolds stresses and the mean shear where the total energy of k_L and k_T is constant, which means that when transition occurs, the energy is transferred from k_L to k_T. The three additional transport equations for k_T, k_L and ω are given as:

$$\frac{Dk_T}{Dt} = P_{k_T} + R_{BP} + R_{NAT} - \omega k_T - D_{k_T} + \frac{\partial}{\partial x_j}\left[\left(\nu + \frac{\alpha_T}{\sigma_k}\right)\frac{\partial k_T}{\partial x_j}\right] \tag{5}$$

$$\frac{Dk_L}{Dt} = P_{k_L} - R_{BP} - R_{NAT} - D_L + \frac{\partial}{\partial x_j}\left[\nu\frac{\partial k_L}{\partial x_j}\right] \tag{6}$$

$$\frac{D\omega}{Dt} = C_{\omega 1}\frac{\omega}{k_T}P_{k_T} + \left(\frac{C_{\omega R}}{f_W} - 1\right)\frac{\omega}{k_T}(R_{BP} + R_{NAT}) - C_{\omega 2}\omega^2 + C_{\omega 3} f_\omega \alpha_T f_W^2 \frac{\sqrt{k_T}}{d^3} + \frac{\partial}{\partial x_j}\left[\left(\nu + \frac{\alpha_T}{\sigma_\omega}\right)\frac{\omega}{x_j}\right] \tag{7}$$

The various terms in the model equations represent production, destruction, and transport mechanisms, where P_{k_T}, D_{k_T} are respectively the production and destruction of turbulent kinetic energy, R_{BP}, R_{NAT} represent the effect of bypass and natural transitions, C_ω, and σ_ω are model constants, f_ω, f_W are the damping functions, and α_T is the effective diffusivity. The detailed definitions of the above terms can be found in [14].

2.4. Solution strategy

The SIMPLE (Semi-Implicit Method for Pressure Linked Equation) algorithm is adopted for the pressure and velocity coupling. Second-order upwind schemes are used for the discretization of momentum and turbulence terms. Moreover, the Moving Reference Frame (MRF) approach is employed to handle the rotation of the propeller. The MRF method is a steady-state approximation for the analysis of situations involving domains that are rotating relatively to each other. The governing equations for the flow in the selected rotating zone are solved in a relative rotating frame. To characterise the performance of the propeller, the following hydrodynamic coefficients are defined:

$$J = \frac{v_a}{nD}, \tag{8}$$

$$K_\mathrm{T} = \frac{\mathrm{T}}{\rho n^2 D^4}, \tag{9}$$

$$K_\mathrm{Q} = \frac{\mathrm{Q}}{\rho n^2 D^5}, \tag{10}$$

$$\eta = \frac{J}{2\pi}\frac{K_\mathrm{T}}{K_\mathrm{Q}}, \tag{11}$$

$$C_p = \frac{p - p_\infty}{\frac{1}{2}\rho v^2}, \tag{12}$$

$$C_f = \frac{\tau_w}{\frac{1}{2}\rho v^2}, \tag{13}$$

which represent the advance coefficient, the thrust and torque coefficients, the efficiency, the pressure and the skin friction coefficients respectively. The representative velocity $v = \sqrt{v_a^2 + (0.7\pi nD)^2}$, v_a is the advance velocity, T is the torque, D the propeller diameter, n the rotational speed and the shear stress $\tau_w = \mu\frac{\partial u}{\partial y}\big|_{y=0}$, with u the flow velocity along the blade surface and y is the normal distance.

3. RESULTS AND DISCUSSION

3.1. Test cases

3.1.1. Flow over a flat plate

To test the capabilities of the $\gamma - Re_\theta$ and $k - k_L - \omega$ transition models, a benchmark test case is examined, namely the flow over a flat plate without pressure gradient. The computational domain and boundary

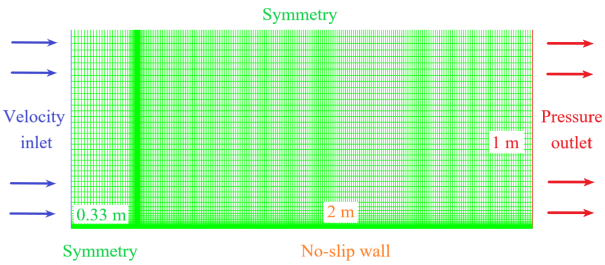

Figure 3. Definition of computational domain, mesh and boundary conditions

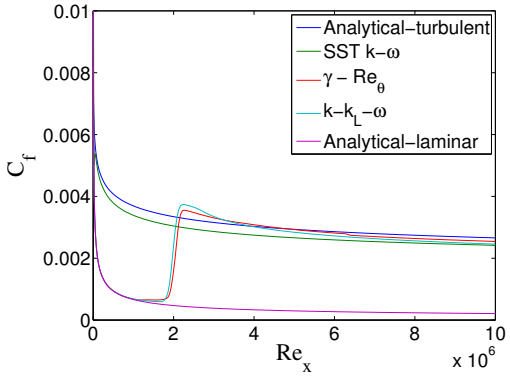

(a) TI=1%, TVR=10

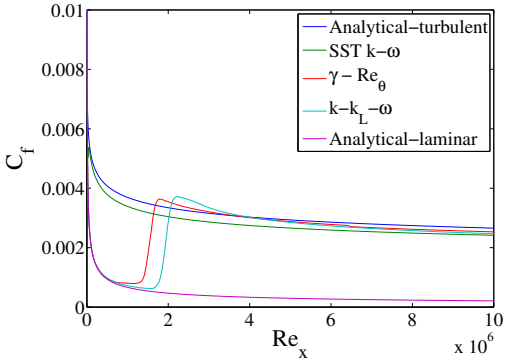

(b) Tu=1%, TVR=100

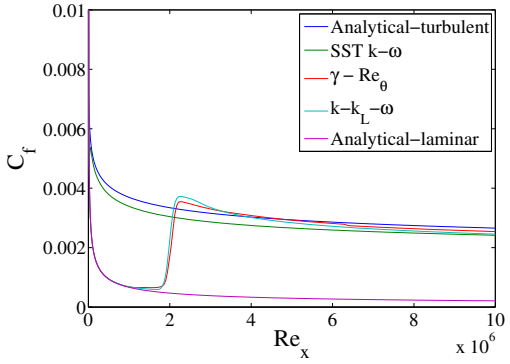

(c) TI=5%, TVR=10

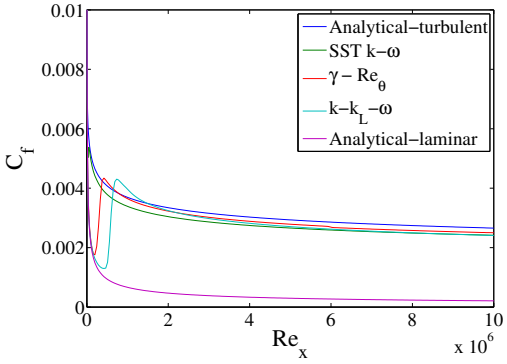

(d) Tu=5%, TVR=100

Figure 4. Influence of inlet parameters on the onset of transition process on a flat plate

conditions are shown in Figure 3. The flat plate has a length of 2 m and is placed 0.33 m downstream the inlet, as indicated by the black circle. A symmetry boundary condition is used to guide the uniform flow from the inlet to the plate. A pressure outlet is adopted at the end of the plate, while a no-slip boundary condition is used for the plate itself.

The transition onset is generally based on the disturbance strength in the boundary layer, which is determined by the flow properties of the free-stream, like turbulence intensity (TI). When the flow develops, there would be a decay in TI, and the turbulent viscosity ratio (TVR) reflects the decaying speed. Therefore different combinations of turbulent intensity and turbulent viscosity ratio are assessed and the results are given in Figure 4. Re_x is the Reynolds number determined by the position on the plate along the flow direction. In this figure, the gray and blue lines represent the analytical solutions for laminar and turbulent flows respectively. From the results it is observed that the values for turbulent intensity and turbulent viscosity ratio can influence the location of transition onset. Because higher turbulent viscosity ratio will reduce the decay of the turbulent intensity, resulting in an earlier onset of the transition process. Therefore, to accurately evaluate a solution for a practical problem, appropriate assessment of there values at the inlet is very important. Generally both transition models can robustly reflect the flow physics.

3.1.2. Open water performance of a ducted propeller

Another test case is conducted for a ducted propeller, where open water tests are available. Figure 5 provides a comparison between the two transition models and experimental measurements obtained from [15]. A good correlation is found between both

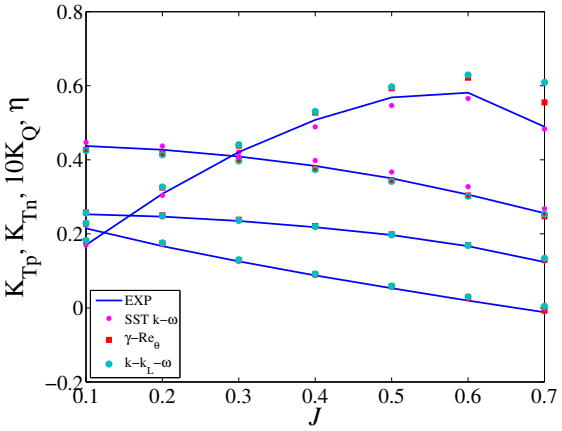

Figure 5. Comparison of open water performance of the ducted propeller between CFD results and experimental data

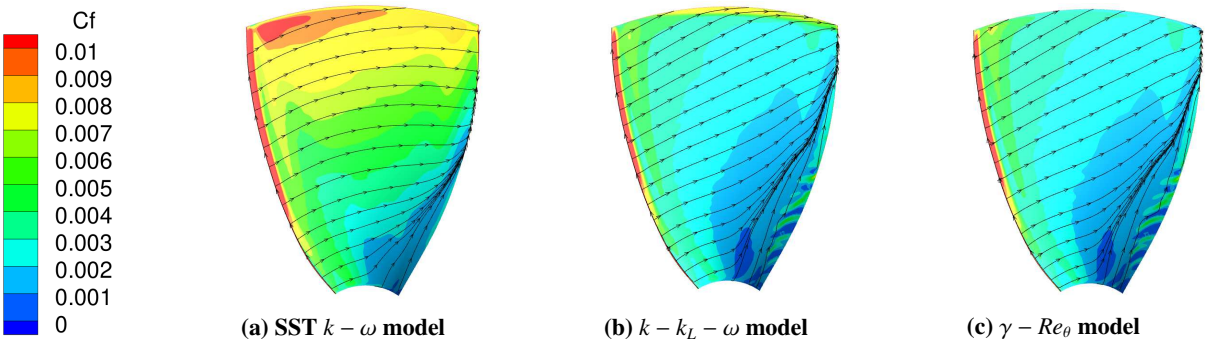

(a) SST $k-\omega$ model **(b) $k-k_L-\omega$ model** **(c) $\gamma-Re_\theta$ model**

Figure 6. Comparison of flow patterns on the blade surface using different models

transition models and experimental data. It is noted that the propeller and duct thrust predicted by the $\gamma - Re_\theta$ transition model are quite close to those obtained by the $k-\omega$ SST turbulence model. The major difference is found for the propeller torque prediction, where the $k-\omega$ SST model gives higher values for propeller torque under all advance coefficients. To find out the reasons, the components of thrust and torque are compared respectively as provided in Table 1, which gives a comparison between the result from the $k-\omega$ SST model and the $\gamma - Re_\theta$ model. It can be observed that pressure is the dominating factor both in thrust and torque and that the difference in torque prediction between the two models is mainly caused by the shear stress. As the transition model gives lower values for skin friction, a slightly higher thrust and a lower torque are expected.

3.2. Open water performance of the RDT

In this section, the simulation results using the fully turbulent and transition models are presented and analyzed for the open water performance of an RDT. To better understand the transition process, different propeller speeds are considered as the Reynolds number needs to be high enough to trigger the transitional effects in the model. Revolution rates of 10 rps and 20 rps are investigated and the Reynolds number at the propeller section of $r/R = 0.7$ is 5.07×10^5 and 1.14×10^6 respectively.

3.2.1. Flow patterns on the propeller

The distribution of skin friction coefficient C_f on the pressure and suction side of the propeller blade with constrained streamlines by all three models is provided in Figure 6. The pattern of the streamlines

Table 1. Contribution of pressure and shear forces to the thrust (T) and torque (Q) of the propeller at $J = 0.1$

	SST $k-\omega$ model		$\gamma - Re_{\theta t}$ model	
	T (N)	Q $(N \cdot m)$	T (N)	Q $(N \cdot m)$
Pressure	93.31	3.69	93.76	3.73
Shear	-1.94	0.41	-0.86	0.17
Total	91.37	4.1	92.9	3.9

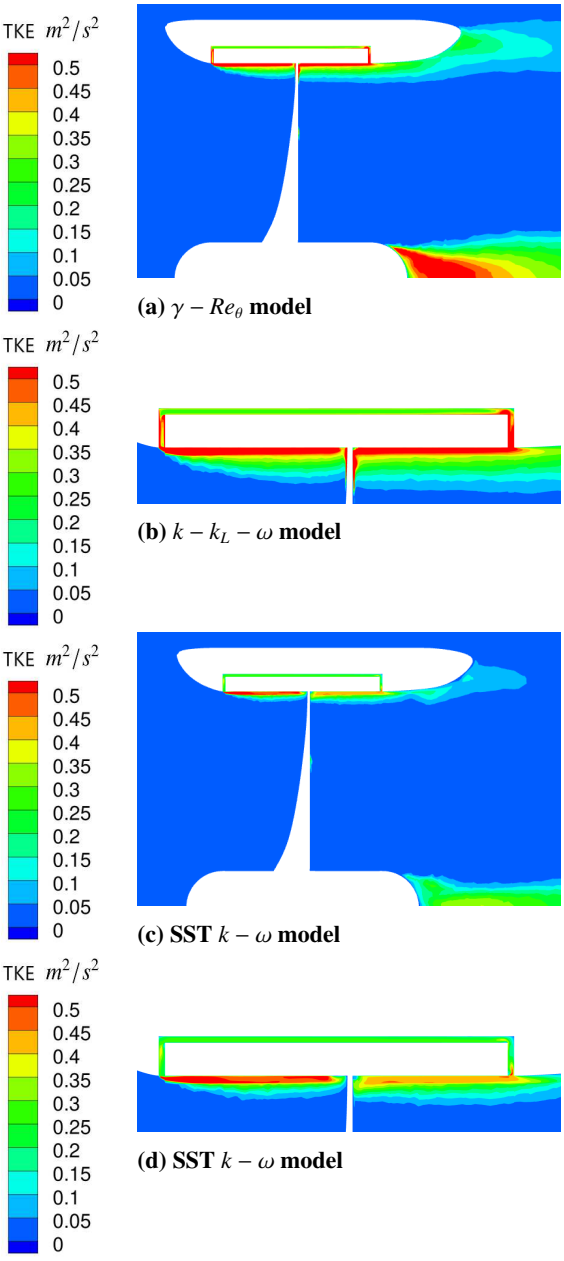

(a) $\gamma - Re_\theta$ model

(b) $k-k_L-\omega$ model

(c) SST $k-\omega$ model

(d) SST $k-\omega$ model

Figure 7. Comparison of turbulent kinetic energy (TKE) distribution near the propeller using the $k-k_L-\omega$ and $\gamma - Re_{\theta t}$ model

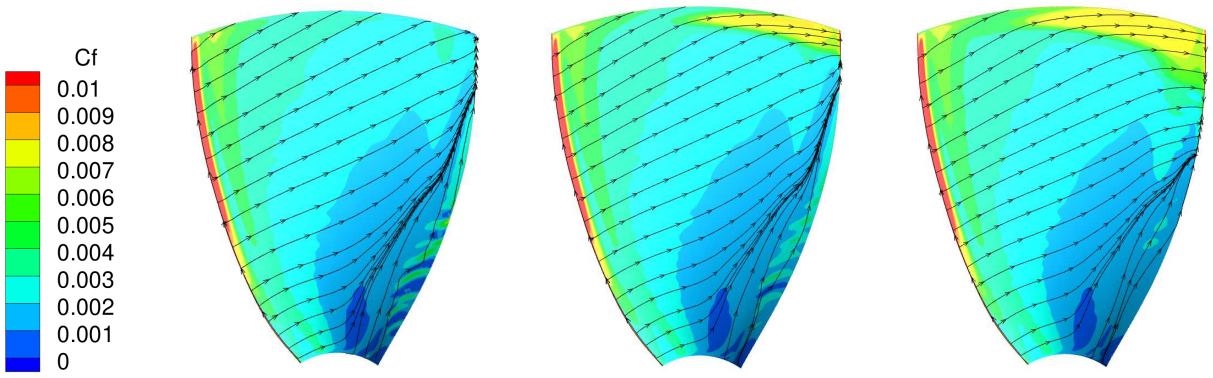

(a) TI=5% and TVR=10 **(b) TI=5% and TVR=100** **(c) TI=5% and TVR=200**

Figure 8. Influence of TI and TVR on the transition process using the $\gamma - Re_\theta$ model

is an indication of the flow regime over the blade. As the direction of the streamline is a result of inertial and centrifugal force, the streamline is always deflected to the dominant force. When the flow is turbulent, the inertial force has greater influence compared to the centrifugal force, therefore the streamline is forced to go along the tangential direction over the blade. However, in the case of a laminar flow, the opposite phenomenon can be observed, and the streamline is outwardly oriented.

The difference in streamline patterns can be clearly observed between the turbulence model and transition models. Moreover, the skin friction is obviously larger in the turbulent flow than in the laminar flow. Because a greater wall shear stress is achieved in the turbulent boundary layer, where the velocity gradient at the wall is steeper. The skin friction distribution on the blade surface predicted by two transition models are quite close, except the difference found at the blade tip. The $k - k_L - \omega$ models gives higher values for C_f, and there is obviously a change in the direction of the streamlines, indicating the flow is changing from a laminar to a turbulent regime. Figure 7 provides a comparison of kinetic energy distribution near the blade by two transition models. There is clearly more turbulent kinetic energy (TKE) production at the blade tip region by the $k - k_L - \omega$, resulting in the change in flow regime. In Table 2, the thrust and torque of different components predicted by two models are compared. The $\gamma - Re_\theta$ model gives higher values for propeller thrust and torque in both pressure and shear forces. However, since there is currently no experimental data available for the RDT, it is hard to conclude which model has higher accuracy in performance prediction.

Table 2. Contribution of pressure and shear forces to the thrust (T) and torque (Q) of the propeller at $J = 0.5$

	$k - k_L - \omega$ model		$\gamma - Re_{\theta t}$ model	
	Pressure	Shear	Pressure	Shear
T_p (N)	26.832	-0.568	31.388	-0.556
T_d (N)	1.512	-0.488	0.808	-0.368
T_r (N)	6.028	-0.564	6.82	-0.248
Q_p $(N \cdot m)$	0.692	0.048	0.792	0.06
Q_r $(N \cdot m)$	0	0.5	0	0.464

3.2.2. Influence of Reynolds number

As discussed above, the turbulence model assumes the boundary layer on the blade is always fully turbulent, despite the fact that there might be transitional flows locally. By comparison, the transition models have the potential to capture this phenomenon. However, it is also observed in previous work that the streamlines are almost all directed outwardly, i.e. the the flow is in laminar regime over the entire blade surface. And this also explains the negligible difference in performance prediction when changing the TI and TVR values at the inlet. As the Reynolds number is below the critical value, the transitional effects are not yet activated. Therefore, to further investigate how the onset of transition is related to the turbulent intensity, a higher rotational propeller rotational rate is considered.

The influence of turbulence intensity of the freestream on the transition process on the blade surface is presented in Figure 8. Three combinations of TI and TVR values are investigated. The TI at the inlet is set constant, therefore the fluctuations close to the thruster are based on the TVR. The higher values of TVR reduce the decay of TI, resulting in an earlier onset of transition. It is clearly observed that with the increase of TVR, the turbulent effect becomes more pronounced at the blade tip, which is indicated by a larger skin friction. It is also noted that the $k - k_L - \omega$ model is not as sensitive to these inlet parameters as the $\gamma - Re_\theta$, and the skin friction distribution and streamline pattern are very close under different disturbances.

4. CONCLUSION

Laminar to turbulent transition flows are often observed on marine propellers at model scales. Accurately resolving this flow phenomenon can significantly improve the performance prediction of the

propeller. In this work, the capabilities of the $k - k_L - \omega$ and $\gamma - Re_\theta$ transition models implemented in the ANSYS Fluent flow solver are tested for the performance prediction of a rim-driven thruster. Different test cases are firstly conducted to ensure the quality of the numerical simulations. From the validation study using the ducted propeller, it is concluded that the transition models exhibit better performance than the turbulence model. The predicted thrusts of propeller and duct, which are mainly based on pressure contribution, are quite close using different models. However, the propeller torque is exceptional. When there is a transitional flow, the transition models give lower values for torque due to smaller shear stress prediction. This is a result of the laminar boundary layer and the streamlines in this situation are more outwardly oriented due to centrifugal acceleration. The comparison between the $k - k_L - \omega$ and $\gamma - Re_\theta$ transition models in hydrodynamic performance prediction of an RDT is then conducted. From the results it is found that there is a small difference between the two models. The $k-k_L-\omega$ predicts more local turbulent regions such as the blade tip, and therefore the skin friction is higher in this region than that of the $\gamma-Re_\theta$ model. The $\gamma-Re_\theta$ model predicts higher propeller thrust, especially for the pressure component, but it is at present not certain which model is more accurate. More research is required for verification.

ACKNOWLEDGEMENTS

The authors would like to thank the China Scholarship Council (CSC) for their financial support for the first author (Grant No. 201806950010). The computational resources and services used in this work were provided by the VSC (Flemish Supercomputer Center), funded by the Research Foundation - Flanders (FWO) and the Flemish Government - department EWI.

REFERENCES

[1] Kuiper, G., 1981, "Cavitation Inception on Ship Model Propeller", Ph.D. thesis, Delft University of Technology.

[2] Wang, X., and Walters, K., 2012, "Computational Analysis of Marine-Propeller Performance Using Transition-Sensitive Turbulence Modeling", *J Fluids Eng*, Vol. 134, p. 071107.

[3] Pawar, S., and Brizzolara, S., 2019, "Relevance of Transition Turbulent Model for Hydrodynamic Characteristics of Low Reynolds Number Propeller", *Appl Ocean Res*, Vol. 87, pp. 165–178.

[4] Liu, B., and Vanierschot, M., 2021, "Numerical Study of the Hydrodynamic Characteristics Comparison between a Ducted Propeller and a Rim-Driven Thruster", *Appl Sci-Basel*, Vol. 11, p. 4919.

[5] Yan, X. P., Liang, X. X., Wu, O. Y., Liu, Z. L., Liu, B., and Lan, J. F., 2017, "A Review of Progress and Applications of Ship Shaft-less Rim-Driven Thrusters", *Ocean Eng*, Vol. 144, pp. 142–156.

[6] Dubas, A. J., Bressloff, N. W., and Sharkh, S. M., 2015, "Numerical modelling of rotor–stator interaction in rim driven thrusters", *Ocean Eng*, Vol. 106, pp. 281–288.

[7] Song, B. W., Wang, Y. J., and Tian, W. L., 2015, "Open water performance comparison between hub-type and hubless rim driven thrusters based on CFD method", *Ocean Eng*, Vol. 103, pp. 55–63.

[8] Cai, M. J., Yang, C. J., Wu, S. J., Zhu, Y. S., and Xie, Y., 2015, "Hydrodynamic analysis of a rim-driven thruster based on RANS method", *OCEANS 2015-MTS/IEEE Washington*, pp. 1–5.

[9] Gaggero, S., 2020, "Numerical design of a Rim-driven thruster using a RANS-based optimization approach", *Appl Ocean Res*, Vol. 94, p. 101941.

[10] Cao, Q. M., Z., W. X., H., T. D., and W., H. F., 2015, "Study of gap flow effects on hydrodynamic performance of rim driver thrusters with/without pressure difference", *J Hydrodynam B*, Vol. 30, pp. 485–494.

[11] Liu, B., Vanierschot, M., and F., B., 2022, "Effects of transition turbulence modeling on the hydrodynamic performance prediction of a rim-driven thruster under different duct designs", *Ocean Eng*, Vol. 256, p. 111142.

[12] Menter, F. R., 1994, "Two-Equation Eddy-Viscosity Turbulence Models for Engineering Applications", *AIAA J*, Vol. 32, pp. 1598–1605.

[13] Menter, F. R., Langtry, R. B., Likki, S. R., Suzen, Y. B., Huang, P. G., and Völker, S., 2006, "A Correlation-Based Transition Model Using Local Variables—Part I: Model Formulation", *J Turbomach*, Vol. 128, pp. 413–422.

[14] Walters, D. K., and Cokljat, D., 2008, "A Three-Equation Eddy-Viscosity Model for Reynolds-Averaged Navier—Stokes Simulations of Transitional Flow", *J Fluids Eng*, Vol. 130.

[15] Oosterveld, M. W. C., 1970, *Wake adapted ducted propellers*, H. Veenman & Zonen, Wageningen, The Netherlands.